

Article

Fuzzy Logic-Based Perturb and Observe Algorithm with Variable Step of a Reference Voltage for Solar Permanent Magnet Synchronous Motor Drive System Fed by Direct-Connected Photovoltaic Array

Mohamed Redha Rezoug ^{1,*}, Rachid Chenni ²  and Djamel Taibi ¹

¹ Departement of Electrical Engineering, Kasdi Merbah University Ouargla, Ouargla 30000, Algeria; taibi.djamel@yahoo.fr

² MoDERNa Laboratory Mentouri, University of Constantine1, Constantine 25000, Algeria; rachid.chenni@gmx.fr

* Correspondence: redha77.rmr@gmail.com; Tel.: +213-077-271-0414

Received: 17 January 2018; Accepted: 14 February 2018; Published: 22 February 2018

Abstract: Photovoltaic pumping is considered to be the most used application amongst other photovoltaic energy applications in isolated sites. This technology is developing with a slow progression to allow the photovoltaic system to operate at its maximum power. This work introduces the modified algorithm which is a perturb and observe (P&O) type to overcome the limitations of the conventional P&O algorithm and increase its global performance in abrupt weather condition changes. The most significant conventional P&O algorithm restriction is the difficulty faced when choosing the variable step of the reference voltage value, a good compromise between the swift dynamic response and the stability in the steady state. To adjust the step reference voltage according to the location of the operating point of the maximum power point (MPP), a fuzzy logic controller (FLC) block adapted to the P&O algorithm is used. This allows the improvement of the tracking pace and the steady state oscillation elimination. The suggested method was evaluated by simulation using MATLAB/SimPowerSystems blocks and compared to the classical P&O under different irradiation levels. The results obtained show the effectiveness of the technique proposed and its capacity for the practical and efficient tracking of maximum power.

Keywords: photovoltaic pumping; MPPT; fuzzy logic control; modified P&O algorithm; variable step

1. Introduction

The electrical energy use is an important demand of our daily life that keeps on growing. Thus, the increase in the electrical energy production is linked to the value of the consumption and the increase in consumption cannot be completely stopped. To remedy that, we boost the systems' efficiency. In addition, the solar energy production via photovoltaic (PV) cells is a very interesting renewable source that should be used to meet the demand for electrical energy.

The abundance and risk-free nature of photovoltaic energy has increased its widespread use until it arrived at an annual growth rate of 35–40% [1].

Recently, photovoltaic energy has caught a lot of interest because its benefits include relatively modest and low complexity structural requirements that are harmless to our planet and renewable compared to standard energy sources. The use of photovoltaic systems allows us to improve the living conditions in remote areas while preserving a clean environment. Last year, photovoltaic systems were installed all around the world. As an example, in 1993, around 10,000 photovoltaic systems were installed for water pumping, and after five years, the photovoltaic systems increased in number six-fold to almost 60,000 systems [2].

The photovoltaic system is constituted of elements that are interconnected and created to achieve the specific purpose and to provide the required electricity by the use of a device related to the load conditions.

The efficiency range may decrease during the fluctuation in: solar radiation, panel temperature conditions, and load. For this, many scientists have examined different maximum power point tracking (MPPT) techniques that were discussed by designers to study control methods and power converters for the tracking of the MPP of a photovoltaic module and extract their disadvantages and advantages so as to understand better their influence on the system's performance.

Lately, for the automatic identification and exploitation at a MPPT, various methods and techniques have been published that differ in many degrees (complexity, yield, cost, material, popularity, speed of convergence, etc.).

A comparison between several aspects of the principal MPPT techniques (CV, P&O, INC, SC, and OV) was discussed in [3–5]. Among the drawbacks of the CV technique (constant voltage) [3] is the negligence of its purpose, which is the tracking of the MPP that was visible when it set the reference voltage to a better fixed voltage and kept it constant under any operating condition, but this technique is also advantageous compared to the P&O (perturb and observe) and INC techniques (incremental conductance), since it overcomes them in efficiency when it is a photovoltaic network of a feeble irradiation and a low implementation cost.

The fact that the OV (fractional open-circuit voltage) and SC (fractional short-circuit current) techniques use an additional static switch to perform the open-circuit and short-circuit conditions makes them more moderate and efficient in energy gains compared to the CV technique. The triviality of the static switches made the authors in [3,5] prefer the P&O and INC techniques for their lower relative cost. In reference [5], the author shows that the P&O techniques implantation cost is more economical than the INC technique's despite the similarity of their performances.

In [6–8] the authors deduced that the P&O method is the most commonly used technique in practice, due to its ease of implementation of a low-cost device. The P&O method has a high MPP tracking performance compared to other techniques. However, it loses this characteristic during quick changes of irradiation and temperature. When weather conditions change slowly or constantly, the algorithm also oscillates around or near the MPP, wasting an amount of the available energy [9].

In this work, a drive system of variable speed consists of a set of interacting elements such as: the photovoltaic panels, the voltage inverter, the permanent magnet synchronous motor (PMSM), and the centrifugal pump. The motor, the space vector pulse width modulation (SVPWM) control, the PV model, and the P&O algorithm will be explained in detail. To improve the drive system in both dynamic response and steady-state, a variable step of reference voltage with P&O algorithm can be implemented using a fuzzy logic controller (FLC).

The collaboration of the system's various elements (motor, P&O algorithm, FLC, and drive system) will be analyzed in terms of performance under different operating conditions such as the irradiation and variation. The results are acquired using MATLAB/Sim-Power-System blocks.

2. Modeling of the Photovoltaic Cells

The modeling of photovoltaic cells resembles the modelling of a current generator mounted in parallel with a diode, as shown in Figure 1. The cell behaves like a diode when there isn't any light to generate the current. As the incident light intensity increases, the cell generates a current.

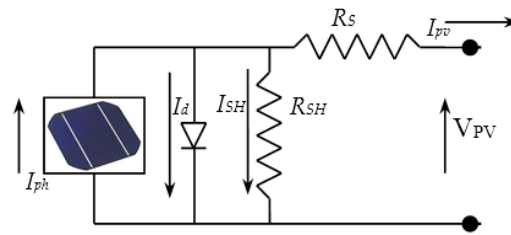


Figure 1. The electrical modeling of the photovoltaic (PV) cell.

The characteristic equation can be deduced directly by using the Kirchhoff law: [10,11]

$$I_{PV} = I_{ph} - I_d - I_{SH} \quad (1)$$

The expansion of the equation connecting the current delivered by a PV module, which consists of putting N_S cells in series and the voltage at its terminals and several variables (as summarized in Table 1 which gives the simplified circuit model), is represented below and in the associated equations:

$$I_{PV} = I_{ph} - I_S \left[\exp\left(\frac{(R_S \cdot I_{PV} + V_{PV})}{V_t}\right) - 1 \right] - \left(\frac{R_S \cdot I_{PV} + V_{PV}}{R_{sh}}\right) \quad (2)$$

$$I_d = I_S \left[\exp\left(\frac{(R_S \cdot I_{PV} + V_{PV})}{V_t}\right) - 1 \right] \quad \text{and} \quad I_{SH} = \left(\frac{R_S \cdot I_{PV} + V_{PV}}{R_{sh}}\right) \quad (3)$$

$$I_{ph} = N_p \cdot I_{ph,cell}, \quad I_S = N_p \cdot I_{S,cell} \quad \text{and} \quad V_t = \frac{N_S \cdot n \cdot k \cdot T}{q} \quad (4)$$

where n is defined as the diode's ideality factor (typically between 1 and 2), and R_S and R_{SH} represent the series and shunt resistors. Manufacturers often tend to supply the R_S value in the datasheet of the product [11]. If not provided, the equation of R_S can be extracted by differentiating the Equation (1) then rearranging it in the R_S phrase.

$$dI_{PV} = 0 - I_S \cdot q \left(\frac{dV_{PV} + R_S \cdot dI_{PV}}{n \cdot k \cdot T} \right) \cdot e^{q \left(\frac{V_{PV} + R_S \cdot I_{PV}}{n \cdot k \cdot T} \right)} \quad (5)$$

$$R_S = - \frac{dI_{PV}}{dV_{PV}} - \frac{n \cdot k \cdot (T/q)}{I_S \cdot e^{q \left(\frac{V_{PV} + R_S \cdot I_{PV}}{n \cdot k \cdot T} \right)}} \quad (6)$$

The solar cells' efficiency is decreased by the power dissipation through the internal resistors during operation. The modeling of these exploitative resistances can be done as that of a parallel shunt resistor (R_{SH}) and a series resistor (R_S). If the R_{SH} decreases too much, the V_{OC} decreases, while the R_S increase may drop the I_{SC} . It is doable to approximate the series values and shunt resistors, R_S and R_{SH} , from the slopes of the I/V curve respectively to the V_{OC} and the I_{SC} . However, the series resistance R_S of the PV module is determined from the 1/slope of the $I-V$ characteristics at open circuit voltage V_{OC} , and the shunt resistance R_{SH} is equal to the inverse of the slope of the $I-V$ characteristics at the short-circuit I_{SC} . After that, the measurements of the resistances to the I_{SC} and the V_{OC} will then be taken and noted.

Table 1. PV Cell Parameters.

Hints	PV Cell Parameters
I_S	Diode saturation current for N_p
$I_{S_{cell}}$	Cell diode saturation current
I_{ph}	Photocurrent for N_p
$I_{ph_{cell}}$	Cell photocurrent
I_{pv}	The output current
I_d	The diode current
I_{SH}	The shunt resistance current
V_t	Thermal voltage for N_s
n	The ideality factor of diode (1.1007)
k	The Boltzmann's constant (1.38×10^{-23} J/K)
T	The $p-n$ junction's temperature
q	The electron's charge (1.6×10^{-19} °C)

Under Matlab/Simulink, the I_{PV} equation was used to define the electrical characteristics of the PV module (Appolo-solar-energy ASEC-205 G6M), as well as to simulate the characteristics of the $P-V$ and $I-V$ for various levels of temperature and irradiation, which are shown in Table 2 by respecting the standard STC's three factors (irradiation, air mass, cell temperature).

Table 2. Manufacturer Specifications for a PV Module.

Parameter	Value
Cell Type	Polycrystalline
Rated Power	$205 \pm 3.0\%$ (W)
Voltage at Maximum Power V_{mp}	25.87 (V)
Open Circuit Voltage V_{oc}	33.58 (V)
Short-Circuit Current I_{sc}	8.61 (A)
Diode saturation current I_d	2.3682×10^{-9} (A)
Current at Maximum Power I_{mp}	7.93 (A)
Temperature Coefficient of V_{oc}	-0.42 (%/°C)
Temperature Coefficient of I_{sc}	0.19 (%/°C)
Cells number per module	6×9
Series resistance R_S	0.43947 (Ω)
Shunt Resistance R_{SH}	116.9171 (Ω)

Figure 2 shows the variation of the $I-V$ and $P-V$ output's characteristics of the simulated PV module as a function of the irradiation and temperature variation. These agree with the characteristics provided by the module manufacturer.

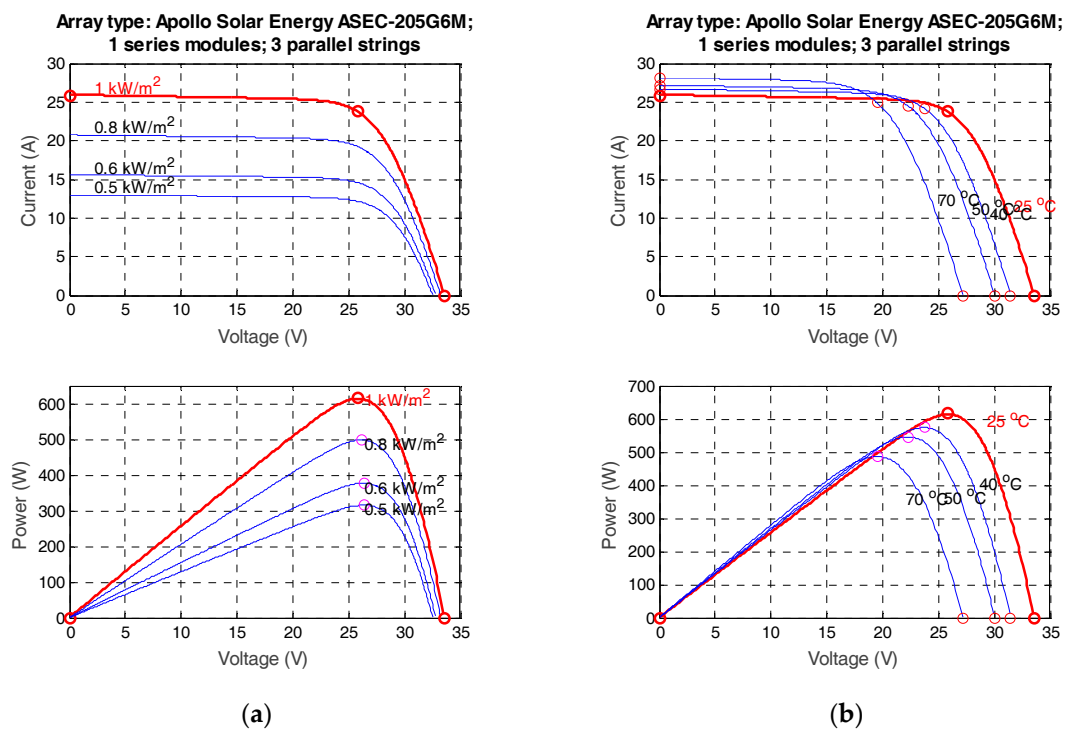


Figure 2. (a) P - V and I - V curves for different irradiance and constant T ; (b) P - V and I - V curves for different temperatures and constant G .

3. Fuzzy Logic-Based P&O Algorithm with Variable Step of a Reference Voltage

The P&O algorithm's basic structure and easy implementation caused it to be considered as the most commonly used MPPT algorithm for all techniques. It is built on the notion that the power-voltage curve dP/dV reaches zero at the curve's top.

Decrementing or incrementing periodically the photovoltaic generator's voltage values or the current output, the corresponding output power comparison of the photovoltaic generator $P(n+1)$, and the previous disturbance $P(n)$ is the P&O's operating principle.

The disturbance has to be maintained in the same initial direction if the disturbance of the terminal voltage causes an increase in the power ($dP/dV > 0$), otherwise it will be moved in the converse direction. This process is redone until the maximum power reaches the point $dP/dV = 0$. We prefer the P&O algorithm for its advantages, but let us not forget its disadvantage, which is the unstoppable oscillation around the power even when it reaches the MPP, which causes extra losses of power. This can be remedied by implementing either a direct duty cycle control where the power is measured at each PWM cycle [12–14], or a reference voltage control where a reference voltage is manipulated as a disturbance parameter and a proportional integral (PI) controller is required to accommodate the duty cycle [15–17].

To eliminate the limitation that exists in the conventional P&O algorithm's implementations, we use a P&O algorithm based on the modified conventional algorithm, in which we implemented a fuzzy logic controller block to provide a variable step of reference voltage. The suggested modified P&O algorithm's flowchart is shown in Figure 3.

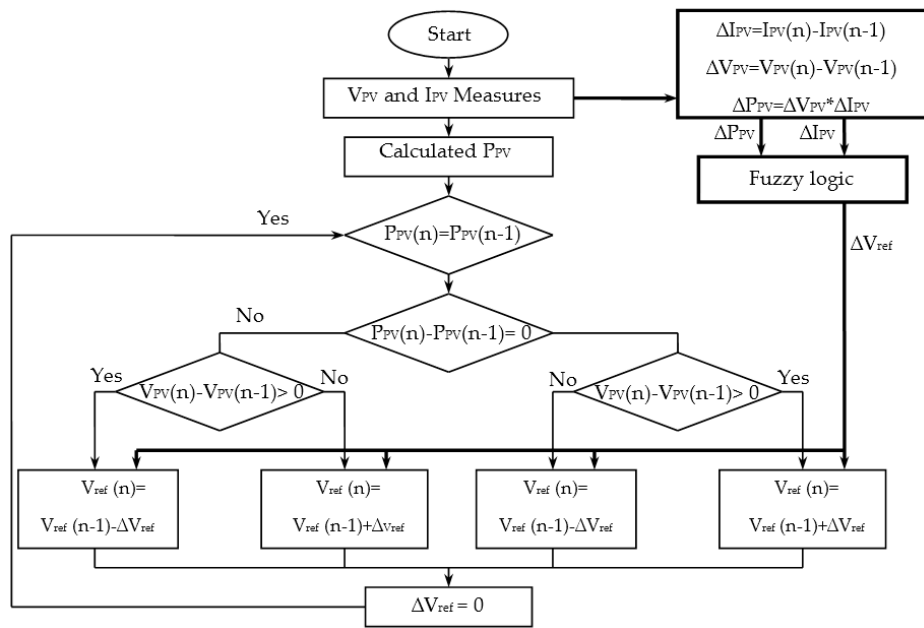


Figure 3. Flowchart of the modified perturb and observe (P&O) algorithm.

The modified power values ΔP_{PV} as well as the modified current values ΔI_{PV} of the photovoltaic generator present the inputs of the fuzzy logic controller block. The adjustments of the controller to the variable step ΔV_{ref} of the P&O depend on the current solar temperature and irradiation. To lower the cost and complexity of the FLC block’s implementation, it is implemented in a way so that it shares the same sensors with the P&O that measure the voltages and currents of the PV generator.

The reference voltage is deemed as a disturbance and control element of the proposed algorithm, so the ΔV_{ref} is disturbed by subtracting or adding the variable step in accordance with the variation of the acquired PV output power. This step is calculated by the adapted FLC block, so it has the role of adjusting the value of the step in accordance with the operating point position. The step value changes proportionally with the interval between the operating point and the MPP. This process continues until the MPP is attained, whose FLC block sets the step value as zero. Therefore, this ensures a fast dynamic response and eliminates the oscillations around the MPP when a steady state is reached.

4. Fuzzy Logic Controller

The fuzzy logic controller proposed is based on an initial knowledge of the system. It is used to modify and control the step of reference voltage. A functional diagram of a FLC block can be structured by collaborating between four sections: fuzzification, inference, defuzzification, and rule base, as illustrated in Figure 4 where the modified values of the photovoltaic generator power ΔP_{PV} and those of the current ΔI_{PV} present the inputs and ΔV_{ref} presents the output that we will send to the P&O algorithm.

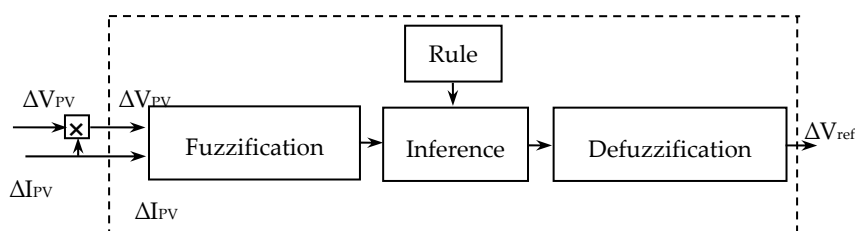


Figure 4. General diagram of a fuzzy logic controller.

The input variables, ΔP_{PV} , ΔI_{PV} , and output ΔV_{ref} of the fuzzy logic controller proposed can be calculated by the use of these equations:

$$\Delta V_{PV}(k) = (V_{PV}(k) - V_{PV}(k - 1)) \tag{7}$$

$$\Delta I_{PV}(k) = (I_{PV}(k) - I_{PV}(k - 1)) \tag{8}$$

$$\Delta P_{PV}(k) = \Delta V_{PV}(k) \times \Delta I_{PV}(k) \tag{9}$$

Using Equations (7) and (8), the power variation values ΔP_{PV} and the output current variation ΔI_{PV} of the PV generator can be stabilized before the fuzzification process to achieve the control calculation's simplification.

In this model, the membership function of the output and input variables used as presented in Figure 5, all membership functions (ΔP_{PV} , ΔI_{PV} , ΔV_{ref}), are expressed with a triangular function. Five linguistic terms are defined: NB as negative big, NS as negative small, ZZ as zero, PS as positive small, and PB as positive big.

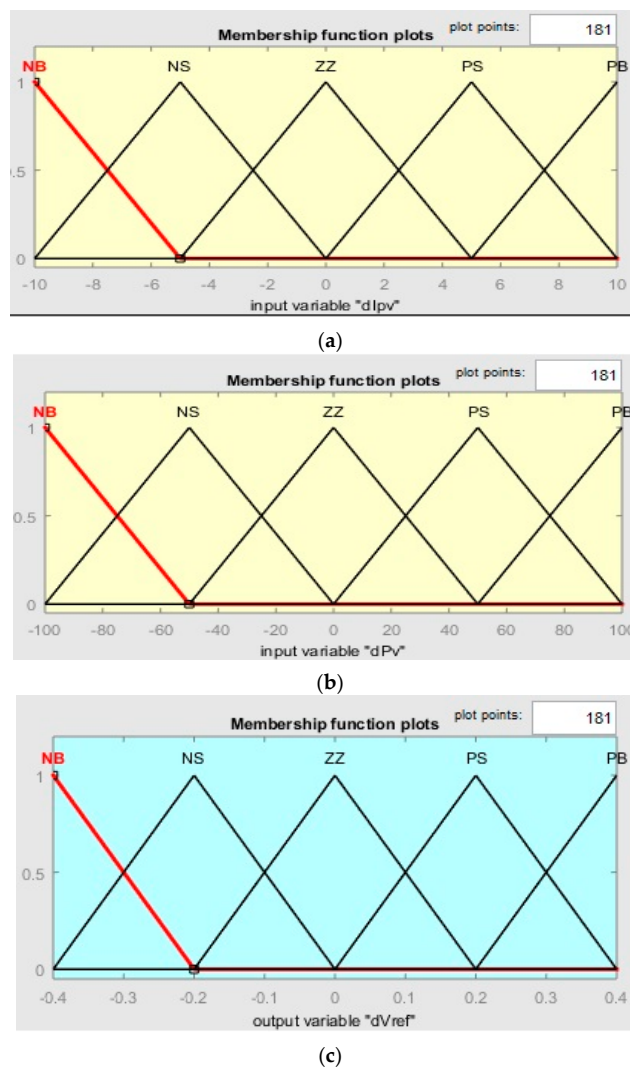


Figure 5. (a,b) Membership functions of the input variables (ΔP_{PV} , ΔI_{PV}) and (c) the output variable ΔV_{ref} .

All information of the monitored parameters are available in the fuzzy rules base that is a set of verification laws (IF THEN). We possess two inputs and each one has five membership functions,

which gives a 25 rule constitution in the FLC inference rules, as given in the Table 3. The function of the latter is to define the variable step of reference voltage so as to convey it to the P&O algorithm to track the PPM and stop iteration once that point is reached.

Table 3. Fuzzy rules base.

ΔI_{PV}	ΔP_{PV}				
	NB	NS	ZZ	PS	PB
NB	NB	NS	NS	ZZ	ZZ
NS	NS	ZZ	ZZ	ZZ	PS
ZZ	ZZ	ZZ	ZZ	PS	PS
PS	ZZ	PS	PS	PS	PB
PB	PS	PS	PB	PB	PB

A fuzzy controller output is always a fuzzy set, so it must be filtered by a defuzzification process to define the net output of the proposed fuzzy control.

Diverse defuzzification techniques were proposed by different authors. In which the defuzzification method of the center of gravity (COG) or centroid [18–20] is the most common, where the shredder determines the gravity center to use its value as an FLC output.

5. Description of Solar Permanent Magnet Synchronous Motor (PMSM) Drive System

5.1. Vector Control of PMSM

One single source composed of three parallel panels is enough to power the PMSM and increase its efficiency. The Kirchhoff voltage law can be utilized so as to express the PMSM voltage equation, as given in the equation:

$$V_d(t) = Ri_d(t) + \frac{d\psi_d(t)}{dt} - \omega_e \psi_q(t) \quad (10)$$

$$V_q(t) = Ri_q(t) + \frac{d\psi_q(t)}{dt} - \omega_e \psi_d(t) \quad (11)$$

where R is the winding resistance of the stator, ω_e is the electrical rotor frequency, and, respectively, ψ_d and ψ_q are the linkage fluxes of the two axis (d -axis and q -axis) when:

$$\psi_d = L_d i_d + \psi_m \quad (12)$$

$$\psi_q = L_q i_q. \quad (13)$$

The ψ_m is the linkage of the flux due to the rotor magnets effects. The electromagnetic torque of a PMSM in the axis d and q can be given by:

$$T_e = \frac{2}{3} p [\psi_d i_d - \psi_q i_q]. \quad (14)$$

The sign p shows the number of pairs of poles. Based on the authors' approach [21], the pole placement method can design the PI controller's parameters. In Figure 6, a global schematic presentation of the PMSM controlled by a vector control powered by an inverter is shown. The desired voltage V_{ref} will be created according to the power generated from three PV panels to consume all the power generated from the panel.

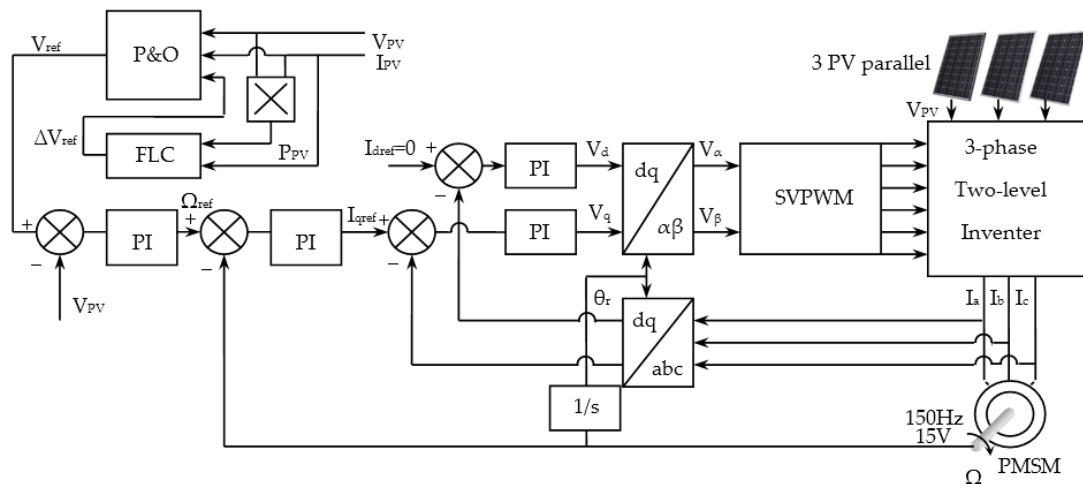


Figure 6. Global schematic of the permanent magnet synchronous motor (PMSM) controlled.

Effectively, after comparing the measured voltage V_{PV} and the desired V_{ref} , the PI controller is added in the outer loop so as to generate the desired Ω_{ref} speed. This latter speed signal is also compared with the measured one as an inner loop. This error signal will be sent to the PI controller, which generates transversal stator current as a reference one. Because the magnets produce a constant flux, the current I_d must be controlled at zero current. PMSM parameters are cited in Appendix A.

5.2. Space Vector Pulse Width Modulation SVPWM

The SVPWM is used in modern drive of electric motors so as to obtain arbitrary waveforms. It will be studied on a three-phase inverter. The concept of the SVPWM consists of reconstructing the voltage vector V_{moy} from eight voltage vectors. Each one of these vectors corresponds to an association of the states of the three-phase voltage inverter switches [20].

A reference voltage vector is calculated globally and approximated over a modulation period T by an average voltage vector V_{moy} . The latter is elaborated by the application of the adjacent voltage vectors and the null vectors V_0 and V_7 . A combinatorial analysis of all the possible states of the switches makes it doable to calculate the voltage vector $(V_{S\alpha}, V_{S\beta})$.

The eight voltage vectors redefined by the association of the switches are represented in the plane (α, β) by Figure 7, [22–25].

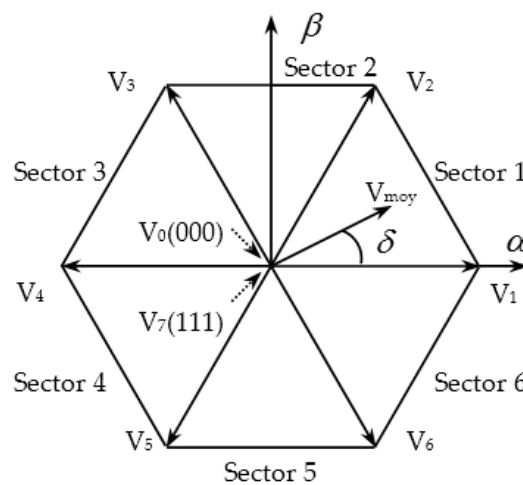


Figure 7. Representation of inverter status and reference voltage vectors in the stationary reference.

5.3. Modeling of the Centrifugal Pump

A pump has a maximum suction (aspiration) capacity, which is the value of the vacuum it can produce. This characteristic differs depending on the type and the pump's technical design.

The centrifugal pump's work involves three parameters: the height, the flow, and the speed. To find the solution of this system of equation, we consider one of the three constant parameters; in general it is the speed which is constant. We have tested our system using a load where the torque increases with the speed squared, such as a pump centrifugal, fan, etc.

$$Tr = k \times \Omega^2 \quad (15)$$

where k is the constant.

6. Simulation Results

The simulation has been done using MATLAB/Sim-Power-Systems blocks as clarified in Figure 8. The modified P&O block requires the V_{PV} and I_{PV} of the PV array to estimate the reference voltage shown in Figure 8. The V_{ref} is compared with V_{PV} and regulated by a PI controller to define the reference speed of the pump motor. The time sampling step of the models of the two blocks (control blocks and power blocks) is taken as 5.14 μ s.

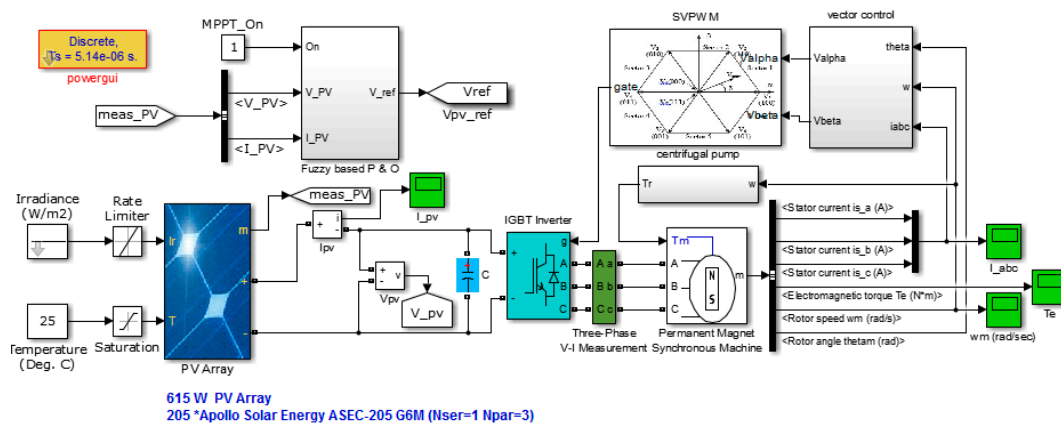


Figure 8. The simulation block diagram of the solar drive systems.

In the first part, a comparative study on the conventional P&O and the P&O based on fuzzy logic is done to show the performance of both techniques under similar conditions. The comparative study takes into consideration two important characteristics: the maximum power point's tracking speed and the oscillation in the steady state. To display the practice of the suggested FLC-based P&O algorithm, this algorithm was tested with two reference voltage steps: 0.01 and 0.05 under two irradiation changes. The irradiation was changed from 1000 to 500 W/m^2 at 0.2 s, then augmented to 1000 W/m^2 at 0.6 s as shown in Figure 9a.

Compared to the P&O with a fixed step of 0.01, the P&O with a fixed step of 0.05 shows a good dynamic performance. It can converge more rapidly to the steady state, but the oscillation is much higher. The dynamic performance of the P&O algorithm can be further improved with a larger step size.

Figure 9b represent variation of voltage reference step size at 0.2 s and 0.6 s. Figure 9c shows that the steady-state oscillation has been totally eliminated in the case of the FLC-based P&O and when the output power of the PV generator is greater than 615 W. In addition, the FLC-based P&O offers a faster dynamic response than the P&O of 0.01 and 0.05.

In the second part, the results of the simulation were obtained to show the performance of the fuzzy logic-based P&O algorithm under different conditions such as quick changes of irradiation.

The results of the drive system of the solar pumping motor are obtained to operate at 25 °C and 1000 W/m². They are given in Figure 10a–d. The power characteristic of the photovoltaic generator is shown in Figure 10a with a maximum power point determined as 615 W. The PV generator’s voltage and current are changed as shown in Figure 10b. It should be known that the PV generator’s voltage is adjusted to the MPP of about 26 V. The three-phase stator currents are given in Figure 10c. The motor speed is changed, as illustrated in Figure 10d, which is limited to the maximum available speed of about 3000 rpm. As a second work, the irradiation is adjusted to 500 W/m². The results are given in Figure 10e–h for this adjusted condition. In this circumstance, the MPP of the PV generator is obtained at about 315 W, as presented in Figure 10e. The photovoltaic generator’s current is decreased from 24 A to 12 A, as illustrated in Figure 10f. Depending on this current decrease, the stator’s currents and the motor speed are decreased as shown in Figure 10g–h. The motor speed is decreased from 2980 rpm to 2250 rpm. The results show that the motor operates at the point of maximum power.

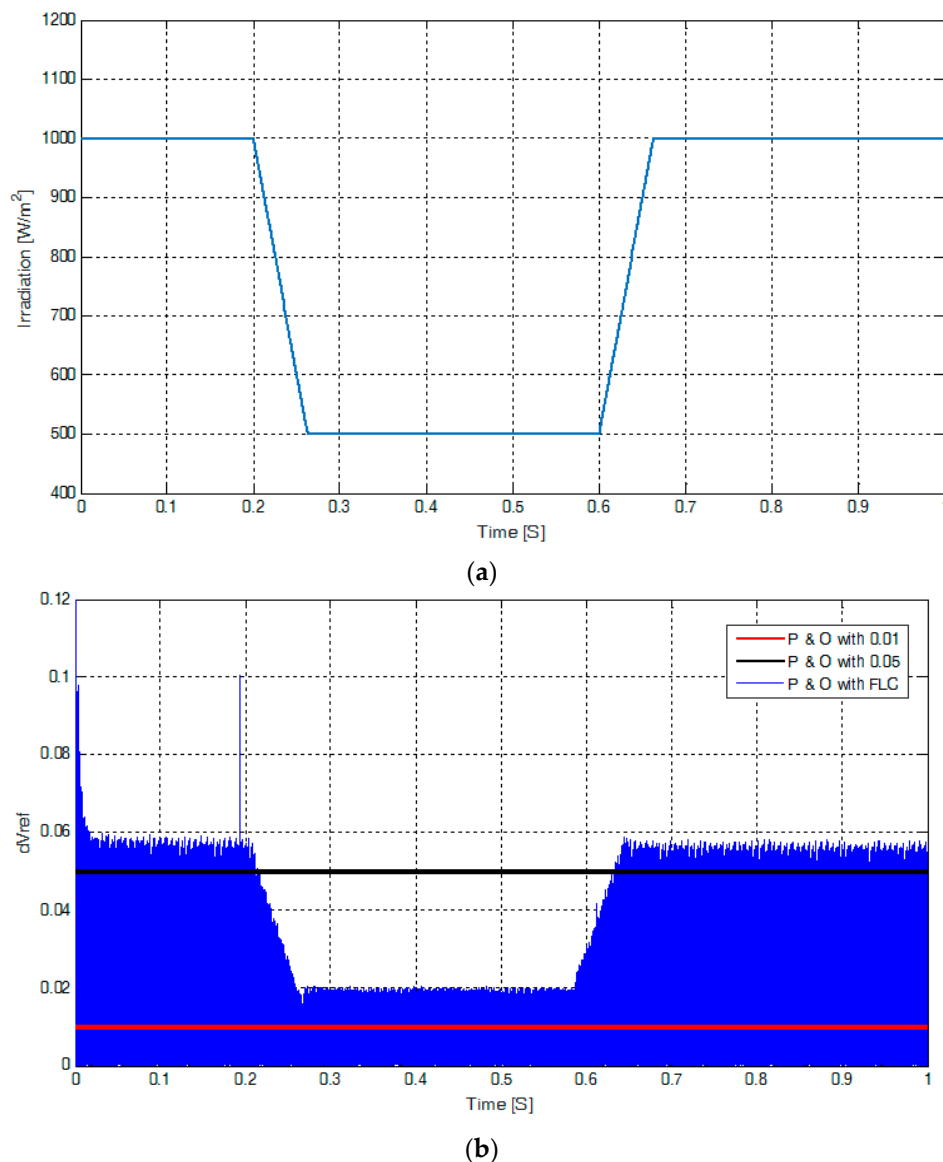


Figure 9. Cont.

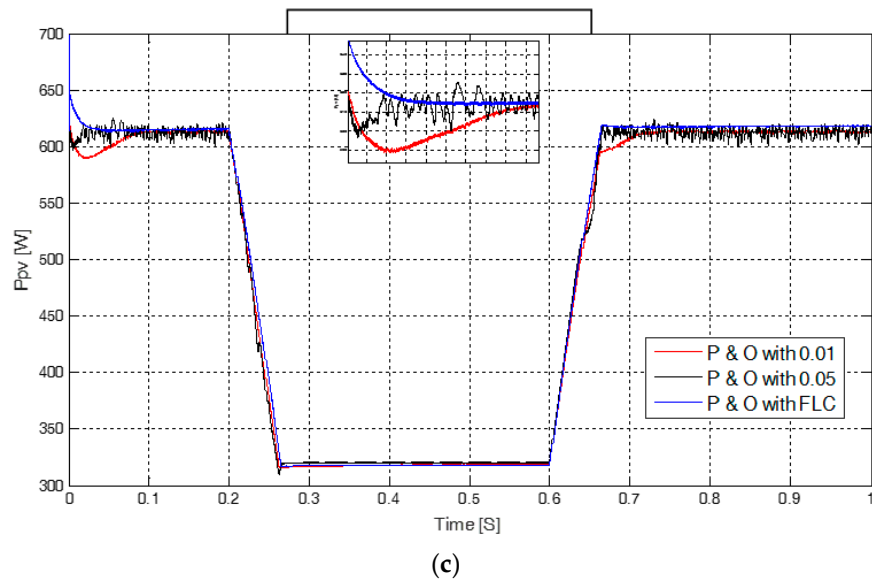


Figure 9. Steady-state and dynamic response comparison of the proposed fuzzy logic controller (FLC)-based P&O with the P&O algorithm with step of reference voltage of 0.05 and 0.01. (a) Changes of irradiation; (b) Variable Step of a Reference Voltage; (c) PV array output power.

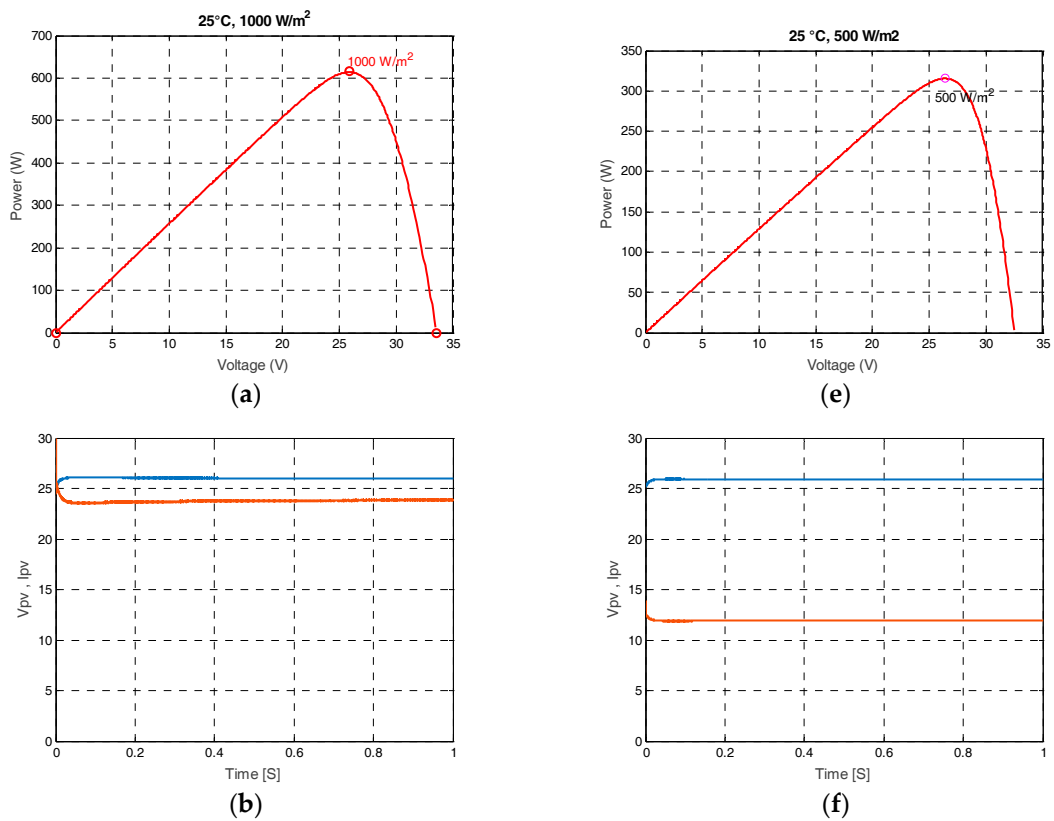


Figure 10. Cont.

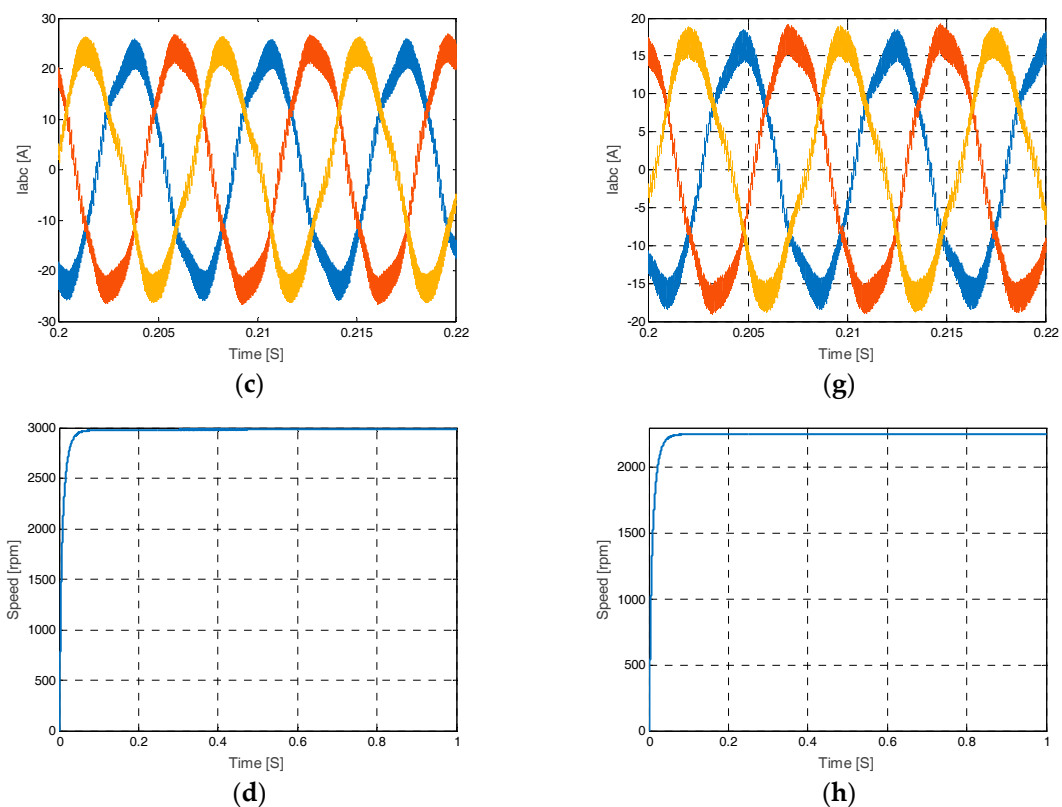


Figure 10. Simulation results of FLC-based P&O algorithm. Operating at 25 °C and 1000 W/m² conditions; (a) *P-V* curve of *PV* array, (b) the *PV* array's current and voltage, (c) Stator currents, (d) Motor speed, operating at 25 °C and 500 W/m² conditions; (e) the *PV* array's *P-V* curve, (f) the parameters (*I*, *V*) of the *PV* array, (g) Stator currents, (h) Motor speed.

7. Conclusions

In this paper, an improvement of the P&O algorithm with the Fuzzy Logic is developed for a permanent magnet synchronous motor (PMSM) drive system to increase the efficiency of the system without the energy storage by a DC/DC converter and batteries. The system is connected directly to the photovoltaic panels. To ensure a nominal power supply of 26 volts for the motor, a minimum of three panels in parallel is sufficient.

For a direct connection to *PV* panels that can generate a low voltage level, a low-voltage PMSM is used. To reduce the torque ripple, we use six poles. Because of the need for a 3000 rpm speed, the nominal frequency of the motor is equal to 150 Hz.

In addition, so as to maximize the power flow between the PMSM and the *PV* array in situations of vigorous radiation and temperature changes, the FLC-based P&O algorithm has been developed. In a changing condition environment, the analysis of the performance of the developed FLC-based P&O algorithm, low voltage PMSM, motor drive, and solar system using MATLAB/SimPowerSystems blocks is performed. The results of the simulation show that at its peak capacity, the pump motor works perfectly even under rapidly changing solar radiation. This proves that the MPPs have been accurately measured with the developed P&O algorithm.

Author Contributions: Mohamed Redha Rezoug, Rachid Chenni, and Djamel Taibi conceived and designed the experiments and performed them; Djamel Taibi and Mohamed Redha Rezoug analyzed the data; Rachid Chenni contributed reagents/materials/analysis tools; Mohamed Redha Rezoug wrote the paper.

Conflicts of Interest: The authors declare no conflict of interest.

Appendix A.

PMSM Parameters;

$V_{dc} = 26$ V; $R = 0,002$ Ω ; $L_d = 786.10^{-5}$ H; $L_q = 102.10^{-4}$ H; $p = 3$; $T_n = 1.8$ Nm; $\psi_m = 0.058$ Wb; $P_n = 415$ W; $I_n = 20$ A; $\Omega_n = 2980$ rpm; $U_n = 15$ V.

References

1. Tyagi, V.V.; Rahim, N.A.A.; Rahim, N.A.; Selvaraj, J.A./L. Progress in solar PV technology: Research and achievement. *Renew. Sustain. Energy Rev.* **2013**, *20*, 443–461. [[CrossRef](#)]
2. Sahin, A.Z.; Rehman, S. Economical Feasibility of Utilizing Photovoltaics for Water Pumping in Saudi Arabia. *Int. J. Photoenergy* **2012**, *2012*, 9. [[CrossRef](#)]
3. Faranda, R.; Leva, S. Energy comparison of MPPT techniques for PV Systems. *WSEAS Trans. Power Syst.* **2008**, *3*, 446–455.
4. Salas, V.; Olías, E.; Barrado, A.; Lázaro, A. Review of the maximum power point tracking algorithms for stand-alone photovoltaic systems. *Sol. Energy Mater. Sol. Cells* **2006**, *90*, 1555–1578. [[CrossRef](#)]
5. Hohm, D.; Ropp, M.E. Comparative study of maximum power point tracking algorithms. *Prog. Photovolt. Res. Appl.* **2003**, *11*, 47–62. [[CrossRef](#)]
6. Piegari, L.; Rizzo, R.; Spina, I.; Tricoli, P. Optimized Adaptive Perturb and Observe Maximum Power Point Tracking Control for Photovoltaic Generation. *Energies* **2015**, *8*, 3418–3436. [[CrossRef](#)]
7. Cabal, C.; Alonso, C.; Cid-Pastor, A.; Estibals, B.; Seguíer, L.; Leyva, R.; Schweitz, G.; Alzieu, J. Adaptive digital MPPT control for photovoltaic applications. In Proceedings of the 2007 IEEE International Symposium on Industrial Electronics, Vigo, Spain, 4–7 June 2007; pp. 2414–2419.
8. Liu, X.; Lopes, L.A. An improved perturbation and observation maximum power point tracking algorithm for PV arrays. In Proceedings of the 2004 IEEE 35th Annual Power Electronics Specialists Conference, Aachen, Germany, 20–25 June 2004; pp. 2005–2010. [[CrossRef](#)]
9. Emilio, M.; Giovanni, P.; Giovanni, S. Two-steps algorithm improving the P&O steady state MPPT efficiency. *Appl. Energy* **2014**, *113*, 414–421. [[CrossRef](#)]
10. Walker, G. Evaluating MPPT converter topologies using a MATLAB PV model. *J. Electr. Electron. Eng.* **2001**, *21*, 49–56.
11. Villalva, M.G.; Gazoli, J.R.; Filho, E.R. Comprehensive Approach to Modeling and Simulation of Photovoltaic Arrays. *IEEE Trans. Power Electron.* **2009**, *24*, 1198–1208. [[CrossRef](#)]
12. Liu, F.; Kang, Y.; Zhang, Y.; Duan, S. Comparison of P&O and hill climbing MPPT methods for grid-connected PV converter. In Proceedings of the 2008 3rd IEEE Conference on Industrial Electronics and Applications, Singapore, 3–5 June 2008.
13. Tan, C.W.; Green, T.C.; Hernandez-Aramburo, C.A. Analysis of perturb and observe maximum power point tracking algorithm for photovoltaic applications. In Proceedings of the IEEE 2nd International Power and Energy Conference, Johor Bahru, Malaysia, 1–3 December 2008.
14. Aashoor, F.A.O.; Robinson, F.V.P. A Variable Step Size Perturb and Observe Algorithm for Photovoltaic Maximum Power Point Tracking. In Proceedings of the 47th International Universities Power Engineering Conference (UPEC), London, UK, 4–7 September 2012.
15. Piegari, L.; Rizzo, R. Adaptive perturb and observe algorithm for photovoltaic maximum power point tracking. *IET Renew. Power Gener.* **2010**, *4*, 317–328. [[CrossRef](#)]
16. Weidong, X.; Dunford, W.G. A modified adaptive hill climbing MPPT method for photovoltaic power systems. In Proceedings of the 2004 IEEE 35th Annual Power Electronics Specialists Conference, Aachen, Germany, 20–25 June 2004.
17. Chihchiang, H.; Chihming, S. Study of maximum power tracking techniques and control of DC/DC converters for photovoltaic power system. In Proceedings of the 29th Annual IEEE Power Electronics Specialists Conference, Fukuoka, Japan, 22 May 1998.
18. Alajmi, B.N.; Ahmed, K.H.; Finney, S.J.; Williams, B.W. Fuzzy-logic-control approach of a modified hill-climbing method for maximum power point in microgrid standalone photovoltaic system. *IEEE Trans. Power Electron.* **2011**, *26*, 1022–1030. [[CrossRef](#)]

19. Musa, S.; Mohd-Radzi, M.A.; Hizam, H.; Abdul-Wahab, N.I.; Hoon, Y.; Mohd-Zainuri, M.A.A. Modified synchronous reference frame based shunt active power filter with fuzzy logic control pulse width modulation inverter. *Energies* **2017**, *10*, 758. [[CrossRef](#)]
20. Deniz, E.; Aydogmus, O.; Aydogmus, Z. Implementation of ANN-based selective harmonic elimination PWM using hybrid genetic algorithm-based optimization. *Measurement* **2016**, *81*, 32–42. [[CrossRef](#)]
21. Wang, Q.G.; Zhang, Z.; Astrom, K.J.; Cheka, L.S. Guaranteed dominant pole placement with PID controllers. *J. Process Control* **2009**, *19*, 349–352. [[CrossRef](#)]
22. Benlarbi, K.; Mokrani, L.; Nait-Said, M.S. A fuzzy global efficiency optimization of a photovoltaic water pumping system. *Sol. Energy* **2004**, *77*, 203–216. [[CrossRef](#)]
23. Mohammed, Y. Design and Implementation of a Robust Current-Control Scheme for a PMSM Vector Drive with a Simple Adaptive Disturbance Observe. *IEEE Trans. Ind. Electron.* **2007**, *54*, 1981–1988. [[CrossRef](#)]
24. Hilloowala, R.M.; Sharaf, A.M. A rule-based fuzzy logic controller for a PWM inverter in a stand alone wind energy conversion scheme. *IEEE Trans. Ind. Appl.* **1996**, *32*, 57–65. [[CrossRef](#)]
25. Farhat, M.; Barambones, O.; Sbita, L. Efficiency optimization of a DSP-based standalone PV system using a stable single input fuzzy logic controller. *Renew. Sustain. Energy Rev.* **2015**, *49*, 907–920. [[CrossRef](#)]



© 2018 by the authors. Licensee MDPI, Basel, Switzerland. This article is an open access article distributed under the terms and conditions of the Creative Commons Attribution (CC BY) license (<http://creativecommons.org/licenses/by/4.0/>).